Khelifati, Nabil; Laine, Hannu S.; Vähänissi, Ville; Savin, Hele; Bouamama, Fatima Zohra; Bouhafs, Djoudi

Dissociation and Formation Kinetics of Iron-Boron Pairs in Silicon after Phosphorus Implantation Gettering

Published in:
Physica Status Solidi (A) Applications and Materials Science

DOI:
10.1002/pssa.201900253

Published: 01/09/2019

Document Version
Peer-reviewed accepted author manuscript, also known as Final accepted manuscript or Post-print

Dissociation and formation kinetics of iron-boron pairs in silicon after phosphorus implantation gettering

Nabil Khelifati[*]*, Hannu S. Laine, Ville Vähänissi, Hele Savin, Fatima Zohra Bouamama and Djoudi Bouhafs*

Dr. N. Khelifati, Dr. D. Bouhafs
Research Center in Semiconductor Technology for the Energetic, Division DDCS, Bd. 2 Frantz Fanon, les sept merveilles B.P.140, 16038 Algiers, Algeria
E-mail: n.khelifati@gmail.com

Dr. H. S. Laine, Dr. V. Vähänissi, Prof. H. Savin
Department of Micro- and Nanosciences, Aalto University, 02150 Espoo, Finland

F. Z. Bouamama
Ferhat Abbas University – Sétif 1, Campus El Bez. 19000 Sétif, Algeria

Keywords: silicon, iron-boron pairs, dissociation-association, phosphorus implantation, gettering

This paper reports the results of a systematic study on the kinetics of dissociation and formation of iron-boron (FeB) pairs in boron-doped Czochralski silicon after phosphorus implantation gettering of iron at different temperatures. The aim of this study is threefold: (i) investigation of the dissociation kinetics of the FeB pairs by a standardized illumination as a function of the iron concentration after gettering process, (ii) study of the kinetics of their association, and (iii) extraction of the characteristic parameters of these two phenomena for gettered samples, in particular the effective time constants of dissociation and association as well as the constant of material, which describes the dissociation rate well in the absence of other recombination channels.

1. Introduction

The contamination of photovoltaic grade crystalline silicon by 3d-transition metals (e.g. Cr, Mn, Fe and Co) that come from feedstock material and also incorporated during processing steps [1], is one of the main solar cell performance-limiting factors. Iron is among the most

detrimental metallic contaminants in silicon because of its ubiquity with a large capture cross section for charge carriers. At high injection level condition, the pairing of iron with shallow dopants like B, In, Ga and Al in p-type silicon, yields further performance degradation because of the significant increase in the capture cross section [2]. In boron-doped crystalline silicon, iron mainly occupies interstitial positively charged sites (Fe_i^+) [3], and because of its high mobility, it tends to form Fe_iB_s pairs with negatively charged substitutional boron (B_s^-) at room temperature [4, 5]. FeB pair dissociation can be carried out by illumination [5], by minority carrier injection [6] or by increasing temperature [7]. The equilibrium state of Fe_iB_s pair formation and dissociation depends on the concentration of boron and the temperature [8, 9].

The study of association and dissociation kinetics in gettered material using phosphorus implantation remains an interesting area, which provides an insight into the local behavior of FeB pairs after Fe gettering through the extraction of corresponding parameters.

This paper presents experimental findings and modeling which give a quantitative description of the light-induced dissociation of FeB pairs and their formation in samples containing P-implanted emitter and which have underwent extended gettering.

2. Experimental

The wafers used in this investigation were p-type Cz-Si single crystalline with a thickness of 380 μm, and a resistivity of ~4 Ω-cm. They are "sister wafers" with virtually identical properties. The oxygen concentration in these wafers is around 10.50 ppma. The Fe-contamination of the wafers was carried out by immersing them in an iron-spiked RCA solution [10]. The iron was diffused into the bulk at 850 °C during an extended period of 50 minutes, in order to ensure a uniform Fe contamination of the bulk with an interstitial iron concentration $[Fe_i]_0 = 1.8 \times 10^{13}$ cm^{-3}. This step was performed in nitrogen ambient containing a small amount of oxygen (5% O_2) to prevent nitride growth on the wafer surfaces. Note that $[Fe_i]_0$ was measured on the

reference wafer with thermal oxide passivated surface. The passivating oxide was grown at 1000°C for 20 minutes after the iron in-diffusion step and wafer cleaning sequence.

The Quasi-Steady State Photo-Conductance (QSSPC) technique was used to determine [Fe_i] by measuring the effective lifetime of the minority charge carriers (τ_{eff}) before and after the complete dissociation of the FeB pairs [11]. Note that the lifetime measurements were carried out at an injection level $\Delta n = 1 \times 10^{15}$ cm^{-3}. The dissociation experiments were made using a powerful xenon flash (50 suns intensity and 2.5 ms period). Using Shockley-Read-Hall (SRH) model, it will be easy to demonstrate that the dissolved iron concentration [Fe_i] is proportional to the difference between the inverse of the lifetimes measured before and after the complete dissociation of FeB pairs [11]. This can be expressed as following:

$$[Fe_i]_{tot} = C\left(\frac{1}{\tau_2} - \frac{1}{\tau_1}\right) \quad (1)$$

where τ_1 and τ_2 are, respectively, the measured carrier lifetimes before the dissociation of FeB pairs (100% FeB) and after their total dissociation (100% Fe_i). The factor C depends on the capture cross sections of FeB pairs and Fe_i, the concentration and the nature of the dopant, the injection level Δn, and the measurement temperature. Its value can be calculated by the simplified SRH model, as described in reference [12].

After the contamination step, the front sides of the wafers were implanted by phosphorus with an energy of 10 keV and a dose of 2.5×10^{15} cm^{-2}. The implanted phosphorus was activated by annealing at 850°C for 20 minutes, and simultaneously both surfaces of the wafer were passivated with thermal oxide layer (SiO_2) growth with a thickness of ~ 28 nm.

Subsequently, the wafers underwent several gettering anneals during cumulative time of 400 minutes at different temperatures: 550 °C, 650 °C, 750 °C and 850 °C. The anneals were carried out under a flow of nitrogen N_2. The heating rate and the cooling rate of anneals were both

10 °C/min. In these experiments the emitter characteristics, i.e. the active phosphorus concentration in the emitter surface $[P^+]_{surf}$ and its sheet resistance R_{sh}, were found to be affected by the anneal temperature. Note that a similar effect is previously reported by Laine et *al.* [10]. **Table 1** shows the values of $[P^+]_{surf}$ and R_{sh} determined, respectively, by electrochemical capacitance-voltage (ECV) and four-point probe measurements, as well as the total interstitial iron concentrations $[Fe_i]_{tot}$ obtained from the measurement of effective lifetime before and after the complete dissociation of FeB pairs.

Table 1. Electrically active phosphorus surface concentrations ($[P^+]_{surf}$) and sheet resistance (R_{sh}) of the emitters, as well as the total interstitial iron concentrations ($[Fe_i]_{tot}$) in the bulk measured from the studied samples.

Anneal temperature (°C)		550	650	750	850
Emitter n^+	$[P^+]_{surf}$ (($\times 10^{19}$ cm^{-3})	1.9	1.1	1.5	4.9
	R_{sh} (Ω/□)	116	126	123	78
Bulk	$[Fe_i]_{tot}$ ($\times 10^{12}$ cm^{-3})	0.72	1.7	1.5	12

The investigation of FeB dissociation kinetics was carried out according to two standard illumination intensities: 1 sun and 0.5 sun by using of a solar simulator setup. Therefore, the temperature of the wafers was regulated and controlled through a thermoelectric cooling system based on the *Peltier effect*. The measurement temperature was set at 25 ± 2 °C.

The evolution of the interstitial iron concentration at given illumination time t can be expressed by the following formula:

$$[Fe_i](t) = C\left(\frac{1}{\tau_2(t)} - \frac{1}{\tau_1}\right) \quad (2)$$

Because $[FeB]_{tot} = [Fe_i]_{tot} = [FeB](t) + [Fe_i](t)$, the normalized FeB pairs concentration defined as $\eta_{FeB}(t) = \frac{[FeB](t)}{[FeB]_{tot}}$ can be also given by:

$$\eta_{FeB}(t) = 1 - \frac{[Fe_i](t)}{[Fe_i]_{tot}} \quad (3)$$

All measurements of $\tau_2(t)$, i.e. $\eta_{FeB}(t)$, were quickly performed by the QSSPC setup, which is installed near the solar simulator equipment. The time required to pull out the wafer from the illumination, measure the lifetime and bring it back under illumination is about 3-4 seconds. For this duration out of illumination, the repairing of FeB cannot takes place because of the slow kinetics of this phenomenon, which usually starts after long period of about 100 seconds without illumination (see data presented below in Figure 5).

3. Results and discussion

3.1. Evolution of the carrier lifetime and the FeB concentration during illumination

Figure 1 shows the variation of the effective lifetime τ_{eff} of investigated samples as a function of illumination time under 1 sun intensity. The $[Fe_i]_{tot}$ values associated to each presented curve are the interstitial iron concentrations determined after complete dissociation of the FeB pairs. The dashed lines represent the maximum values of the lifetime obtained by the flash.

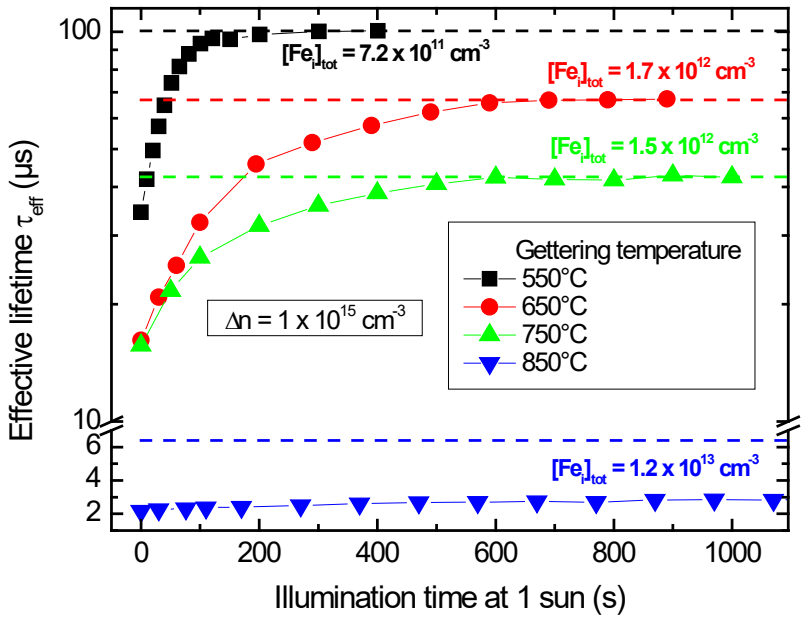

Figure 1. Variation of effective lifetime τ_{eff} versus illumination time at 1 sun for the set of studied samples. Dashed lines represent the maximum values of the lifetime obtained after a complete dissociation of FeB pairs by using a powerful flash.

Because used wafers are B-doped Cz-Si with non-negligible oxygen concentration, which is in the order of magnitude of 10.50 ppma, the Light-Induced Degradation (LID) [13, 14] effects on carrier lifetime have to be discussed. In fact, the results obtained under the conditions of this study do not indicate the dominance of the LID effect on the measured lifetime comparable to that of FeB pairs dissociation. Indeed, the evolution of the lifetime curves with illumination time shows a typical behavior related to the dissociation of the FeB pairs, particularly observed in the presence of the *crossover point (COP)*. The constancy of this crossover point during illumination is robust and convenient "fingerprint" for FeB dissociation, and makes it an excellent identifier of Fe in silicon [12, 15]. This behavior is observed for all samples during the dissociation experiments. Hence, in the following parts we discuss the experimental findings only according to the FeB pairs dissociation.

We remark from the results presented in **Figure 1** that the rate of FeB dissociation varies from one sample to other depending on the temperature anneal, and so also on the total iron

concentration $[Fe_i]_{tot}$. This can be qualitatively observed over the time required to achieve maximum and constant lifetime values. When $[Fe_i]_{tot}$ decreases, this rate gradually increases. Indeed, for the sample gettered at 550 °C and which contains the lowest concentration $[Fe_i]_{tot}$, a complete FeB dissociation (τ_{max} = 100 µs) was reached after 1 sun illumination for ~120 s. In the case of samples treated at 650 °C and 750 °C which contain higher iron concentrations of 1.7×10^{12} cm^{-3} and 1.5×10^{12} cm^{-3}, respectively, the lifetime reached its maximum values after an extended illumination of more than 600 s. For the highly iron contaminated sample (gettered at 850 °C), the result shows that a complete dissociation is far from being achieved even beyond 1200 s of illumination. These findings show that the kinetics of FeB pairs dissociation is significantly affected by the iron concentration $[Fe_i]_{tot}$.

A quantitative exploitation of our results requires the monitoring of the normalized concentration η_{FeB} during the dissociation of the FeB pairs. η_{FeB} is given by [16-18]:

$$\eta_{FeB}(t) = \frac{[FeB](t)}{[FeB]_{tot}} = \left(\frac{R_d}{R_d+R_a}\right) exp[-(R_d + R_a)t] + \left(\frac{R_a}{R_d+R_a}\right) \quad (4)$$

R_d and R_a are, respectively, the dissociation and the association rates of FeB pairs during the dissociation phenomenon.

Figure 2 shows the variation of the normalized FeB concentration $\eta_{FeB}(t)$ as a function of the illumination time for 1 sun and 0.5 sun intensities. The solid and dashed lines represent the fit curves generated by using the **equation (4)**. Note that the dissociation (R_d) and association (R_a) rates were varied in a manner to obtain a quality factor (R^2) closer to 1.

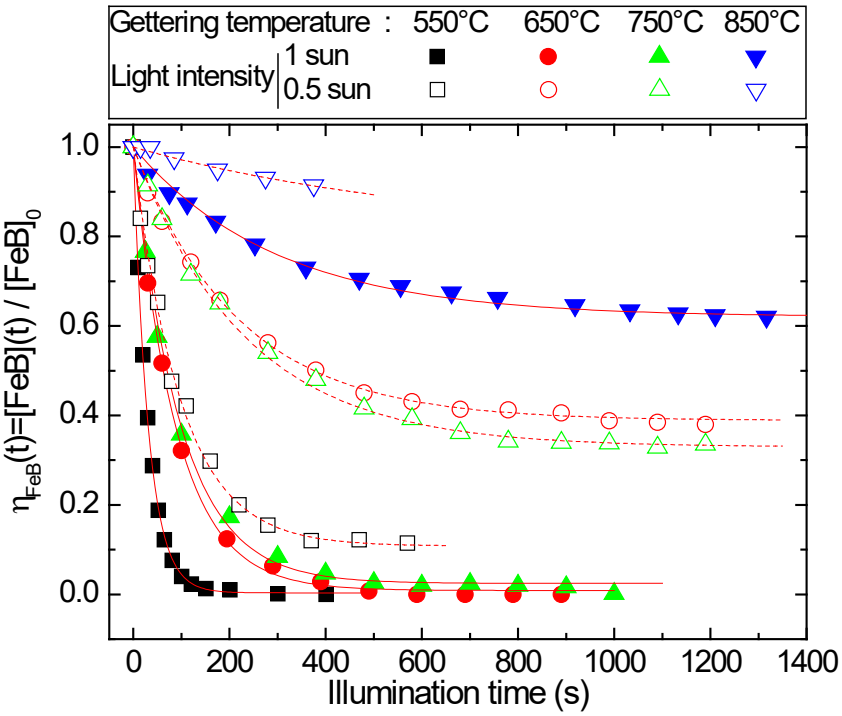

Figure 2. Variation of the normalized FeB concentration $\eta_{FeB}(t)$ for the gettered samples as a function of illumination time under two light intensities: 1 sun (100 mW/cm^2) and 0.5 sun (50 mW/cm^2). The solid and dashed curves in red represent the fitting of experimental data corresponding to 1 sun and 0.5 sun, respectively.

We observe that under the illumination of 1 sun of intensity, the complete dissociation of FeB pairs is more or less rapidly achieved for the samples gettered at 550° C, 650 °C and 750 °C. The dissociation kinetics depends directly from $[Fe_i]_{tot}$ and its rate is limited by the simultaneous FeB repairing. In the case of sample gettered at 850 °C, the dissociation phenomenon is partial because of the high Fe concentration ($[Fe_i]_{tot} = 1.2 \times 10^{13}$ cm^{-3}), which provokes more pairing between iron and boron atoms during the dissociation process. The percentage of dissociated FeB pairs tends to be constant around 40% for an extended illumination period exceeding 1300 s.

Another possible explanation of the partial dissociation of FeB pairs in the sample gettered at 850°C is the low excess carrier density (electron density) associated to high iron recombination activity. This low excess carrier density leads to the decrease in the rate of captured electrons

to form Fe_i^-, which is responsible of the Coulomb repulsion in between the FeB pairs causing then their dissociation: $Fe_i^+B_s^- + 2e^- \rightarrow Fe_i^- + B_s^-$.

The mechanism of FeB dissociation can be described by the capture of two electrons simultaneously to form Fe_i^- [16], or by the capture of the first electron to form Fe_i^0 which eliminate the Coulomb attraction between Fe_i and B_s, followed by the capture of the second electron that triggers the electron-phonon interactions and leads to an athermal diffusion of Fe_i^0 away from B_s^- [6].

The phenomenon of partial dissociation becomes clearer in the case of illumination intensity of 0.5 sun, where the normalized concentration of not dissociated pairs at equilibrium state, i.e. $\eta_{FeB}(t\rightarrow\infty)$, varies considerably from 0.1 to 0.9 when $[Fe_i]_{tot}$ increases from 7.2×10^{11} cm^{-3} and 1.2×10^{13} cm^{-3}, respectively.

3.2. Impact of iron concentration after gettering on dissociation and association rates of FeB pairs

Another interesting observation can also be drawn from the evolution of the curves of $\eta_{FeB}(t)$ as a function of $[Fe_i]_{tot}$ and the illumination intensity. It concerns the variation of the slope of $\eta_{FeB}(t)$ curves in the region of exponential decay associated to $t < 100$ s. The obtained results show that the increase in $[Fe_i]_{tot}$ causes a decrement in this slope, while the increase in illumination intensity has an opposite effect.

According to **equation (4)**, the slope of curve $\eta_{FeB}(t)$ when $t\rightarrow 0$ is equal to the dissociation rate (R_d) of the FeB pairs, and therefore it can be correlated with the "time constant of dissociation τ_{d_eff}" which is defined as $1/(R_d + R_a)$. The dissociation rate R_d is a function of all other phenomena that can accompany the dissociation process (e.g. surface carrier recombination). R_d is given by the following formula [16]:

$$R_d = K \times \left(\frac{G}{[FeB]_{tot}} \times \frac{1}{\left(1+\frac{\tau_{FeB}}{\tau_{other}}\right)} \right)^2 \quad (5)$$

where K is the constant of material that describes the dissociation rate well in the absence of other recombination channels. G is the carrier generation rate in silicon. For an illumination of 1 sun (AM1.5G 100 mW.cm^{-2}), the rate G is close to 8.3×10^{18} cm^{-3}.s^{-1}. τ_{FeB} and τ_{other} are carrier lifetimes limited by recombination activities of FeB pairs and *other defects*, respectively. Note that τ_{other} has been evaluated after the total dissociation of FeB pairs and with using $[Fe_i]_{tot}$. The calculated values of $\frac{\tau_{FeB}}{\tau_{other}}$ obtained for our samples are shown in the following **Table 2**.

Table 2. Values of the τ_{FeB} / τ_{other} ratio obtained for studied samples at $\Delta n = 1 \times 10^{15}$ cm^{-3}.

Anneal temperature (°C)	550	650	750	850
$\frac{\tau_{FeB}}{\tau_{other}}$	1.34	1.15	1.39	1.22

Therefore, for an adequate inspection of only the FeB dissociation kinetics, we introduced the parameter $\tau^*_{d\_eff}$ determined by the following equation:

$$\tau^*_{d\_eff} = \frac{1}{(R^*_d + R_a)}, \text{ where } R^*_d = R_d \left(1 + \frac{\tau_{FeB}}{\tau_{other}}\right)^2 = K \times \left(\frac{G}{[FeB]_{tot}}\right)^2 \quad (6)$$

In the following we present the effect of $[Fe_i]_{tot}$ diminution on the parameters describing the FeB dissociation kinetics; R_d, R_a and effective time constant of dissociation $\tau^*_{d\_eff}$, as well as the constant of material K. The rates R_d and R_a were calculated by fitting of $\eta_{FeB}(t)$ curves, while $\tau^*_{d\_eff}$ and K were determined by using the **equation (6)**.

Figure 3 (a) and **(b)** show the variations of dissociation and association rates as well as the effective time constant of dissociation $\tau^*_{d\_eff}$ as a function of the concentration $[Fe_i]_{tot}$ for 1 sun and 0.5 sun illumination intensity.

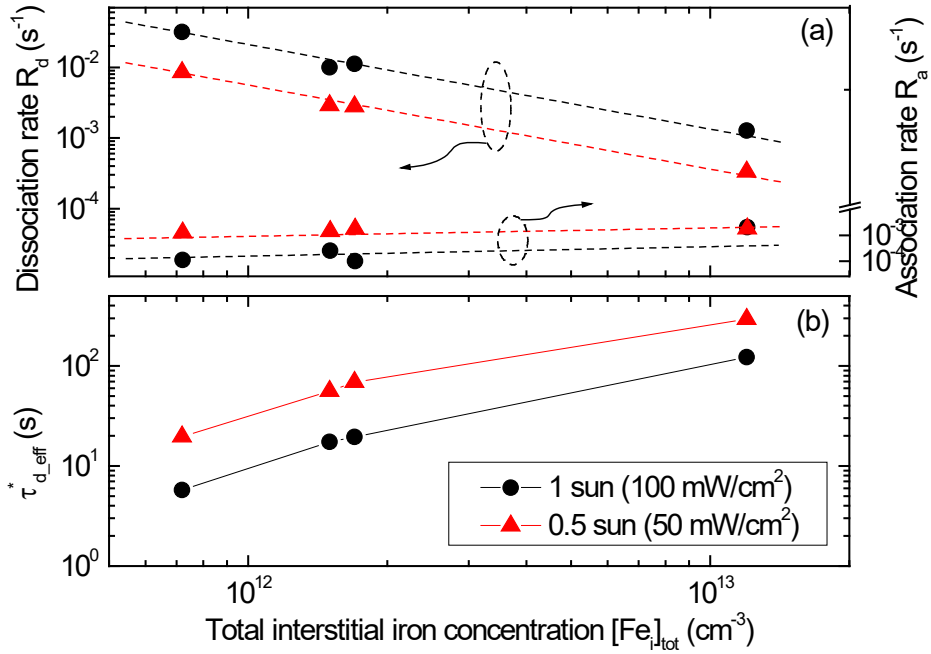

Figure 3. Effect of iron concentration on: (a) dissociation rate R_d and association rate R_a, and (b) the effective time constant of dissociation $\tau^*_{d\_eff}$ for illumination intensities of 1 sun and 0.5 sun.

Note that when $[Fe_i]_{tot}$ varies from 7.2×10^{11} cm^{-3} to 1.2×10^{13} cm^{-3}, the dissociation rate R_d decreases significantly by more than one order of magnitude for both illumination intensities. In contrast to R_d, the association rate R_a tends to increase slightly in the range 10^{-4} – 10^{-3} s^{-1} with the increasing of $[Fe_i]_{tot}$.

The model of FeB pairs formation developed by Kimerling and Benton [6] excludes the association under illumination, because the quasi-Fermi level exceeds the interstitial iron energy level position. Hence, according to this model the interstitial iron is neutrally charged during illumination and no Coulombic attraction between iron and boron occurs. However, the experimental results contradict this theoretical claim. In this context, Möller et *al.* [19, 20] discussed the effect of illumination intensity on the association rate and explained the origin of the appearance of Coulombic attraction between iron and boron even under illumination, by

using an extension of the model developed by Istratov et *al.* [4]. The experimental findings were interpreted in view of the illumination dependent quasi-Fermi level position and the steady state between iron, boron and excess charge carriers. Indeed, if the excess charge carrier density is low compared to the doping concentration, the most likely reaction is that between boron and interstitial iron. If the excess charge carrier density increases, the reaction probability between interstitial iron and boron decreases and the adjusted steady state is shifted to the interstitial iron.

In this present investigation we found that the increasing of non-gettered iron in the bulk that is due to the decreasing of gettering effectiveness causes a decrease in excess charge carriers at fixed illumination intensity. According to the interpretation of Möller et *al.* above, this decrease in excess charge carriers promotes the reaction between boron and interstitial iron which explains the increase in the association rate R_a illustrated in Figure 3(a). Despite the increase of R_a is low under the effect of increasing of iron concentration, this result matches well the model developed by Möller et *al*.

The effect of the iron concentration on the effective time constant of FeB pairs dissociation ($\tau^*_{d\_eff}$) is significant as shown in Figure 3 (b). Indeed, the increase of $[Fe_i]_{tot}$ from 7.2×10^{11} cm^{-3} to 1.2×10^{13} cm^{-3} yields a gradual increase of $\tau^*_{d\_eff}$ from 2 s to more than 122 s for 1 sun intensity, and from 7 s to 293 s for 0.5 sun intensity. These results indicate clearly that the time required for a total dissociation of the FeB pairs becomes more important with the increase of the concentration of the FeB pairs themselves, on the one hand, and the decrease of the illumination intensity, on the other hand.

Another important parameter related to the phenomenon of FeB pairs dissociation by illumination, and which was also determined in this present study, is the constant of material K which is previously presented in **equations (5)** and **(6)**. **Figure 4** shows the values of R^*_d as a function of $\left(\frac{G}{[FeB]_{tot}}\right)^2$ obtained for all samples under 1 sun and 0.5 sun intensities of

illumination. We remark that the data found follow a linear variation, indicating a relationship similar to that expressed by the **equation (6)**.

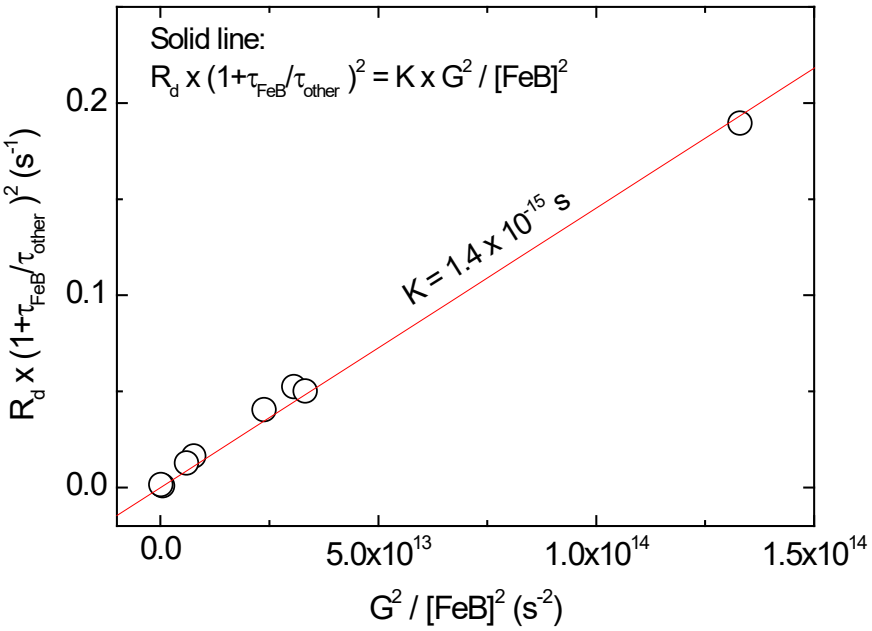

Figure 4. Variation of the dissociation rate R^*_d as a function of $\left(\frac{G}{[FeB]_{tot}}\right)^2$. The red line represents the fit of experimental data using **equation (6)**.

By fitting experimental findings using **equation (6)**, the constant of material K is determined. With a quality of fit $R^2 = 0.97104$, the constant K was found to be 1.4×10^{-15} s. This value of K is between 2.6×10^{-16} s and 5.0×10^{-15} s associated respectively to multicrystalline silicon [17] and monocrystalline silicon [16]. Note that as far as is known, the origin of such variation of the constant K from one type of material to another has not been reported or explained in the literature.

3.3. Kinetics of FeB repairing

In this section, we present the evolution of the FeB pair concentration during their reformation, as well as the effect of the iron concentration $[Fe_i]_{tot}$ on the association rate of Fe_i with B_s. We

note that the monitoring of FeB repairing was started immediately after the dissociation experiments presented above. This study was carried out, as in the case of dissociation, through the measurement of the effective lifetime τ_{eff} as a function of time. After FeB dissociation under 1 sun illumination intensity, the variation of τ_{eff} during association step is shown in **Figure 5 (a)**.

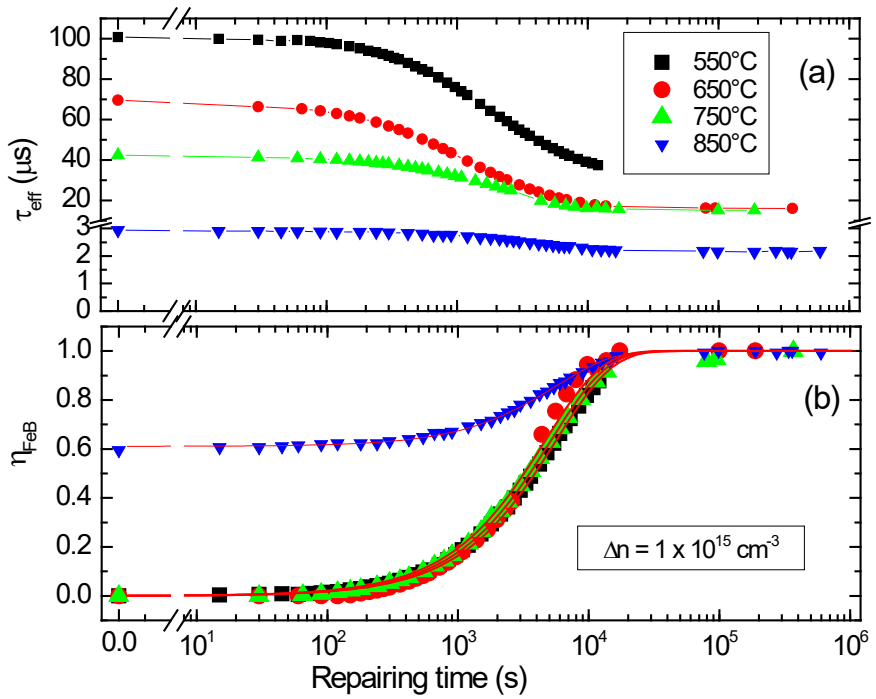

Figure 5. Variation of the effective lifetime τ_{eff} (a) and the normalized concentration η_{FeB} (b) as a function of the association time of the studied samples after an illumination intensity of 1 sun. The solid lines (in red) represent the fitting plots.

One can observe that τ_{eff} follows an exponential decay, indicating that this phenomenon is characterized by an association time constant. Indeed, previous studies published by Reiss et *al.* [21] and Macdonald et *al.* [9] demonstrated that if the iron atoms are homogeneously distributed in the silicon volume with a lower concentration than the dopant density, the Fe_i concentration (*i.e.* τ_{eff} at high injection level) decreases exponentially with a time constant τ_a.

The calculation and the fitting of the normalized FeB concentration (η_{FeB}) during their formation using **equation (7)** below, allowed us to determine the association (R_a) and dissociation (R_d) rates:

$$\eta_{FeB}(t) = \frac{[FeB](t)}{[FeB]_{tot}} = \left(\eta_{FeB}(0) - \frac{R_a}{R_a+R_d}\right) exp[-(R_a + R_d)t] + \frac{R_a}{R_a+R_d} \quad (7)$$

Note that the parameters R_a and R_d studied during the association are different than those corresponding to the dissociation phenomenon reported previously.

The $\eta_{FeB}(t)$ curves and their fitting are illustrated in **Figure 5 (b)**. Because the dissociation of FeB pairs under 1 sun is complete in samples gettered at 550 °C, 650 °C and 750 °C, the association phenomenon starts with $\eta_{FeB}(t=0) = 0$, while in the case of sample gettered at 850 °C, where the dissociation is partial and the beginning of repairing occurred at $\eta_{FeB}(0) = 0.6$.

Since in our work the association experiments were done under normal conditions (room temperature and room light), the dissociation rate R_d can therefore be neglected compared to R_a, *i.e.* $R_a + R_d \approx R_a$. This explains the constancy of final η_{FeB} around 1 ($\eta_{FeB}(t\rightarrow\infty) = 1$).

The extraction of R_a through the fitting of $\eta_{FeB}(t)$ curves illustrated in Figure 5 (b) allowed to study the FeB association kinetics as a function of the $[Fe_i]_{tot}$ concentration after gettering experiment.

Figure 6 shows the experimental R_a values obtained for studied samples, as well as the theoretical plot of R_a, which is the inverse of association time constant τ_a given by the following equation [19, 22]:

$$\tau_a = \frac{\varepsilon\varepsilon_0\, k_B}{q^2} \frac{T}{D(Fe_i)\,.\,N_A} = 5.7 \text{ x } 10^5 \left(\frac{T}{N_A}\right) exp\left(\frac{E_{mig}}{k_B T}\right) \quad (8)$$

where $D(Fe_i)$ is the diffusion coefficient of interstitial iron at temperature T, E_{mig} is the thermal activation energy of the Fe_i migration ($E_{mig} \approx 0.66$ eV), N_A is the boron concentration, ε is the relative dielectric permittivity of silicon, ε_0 is the dielectric permittivity of vacuum, k_B is the Boltzmann constant and q is the elementary electric charge.

It is clear that the experimental findings of R_a remain constant around 1.88×10^{-4} s^{-1}, which is separately calculated for T = 27 °C and $N_A = 4 \times 10^{15}$ cm^{-3}. In contrast to R_d, during the dissociation the R_a corresponding to the association process remains constant and independent of $[Fe_i]_{tot}$. This result confirms those reported in literature [9].

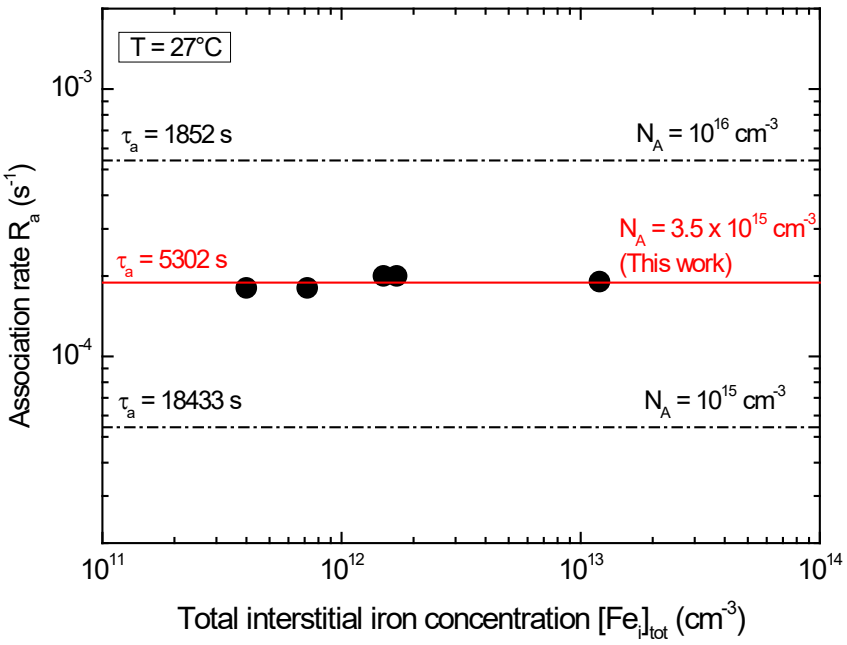

Figure 6. Comparison between the results of R_a found experimentally (black symbols) and obtained by calculation for doping level $N_A = 4 \times 10^{15}$ cm^{-3} associated to studied samples (red line). The dashed black lines represent R_a values for two boron doping levels; 10^{15} cm^{-3} and 10^{16} cm^{-3}.

4. Conclusions

In this work, we reported the results of a systematic study on the FeB dissociation and association kinetics in p-type Cz-Si. The samples used in this study were contaminated with iron at 1.8×10^{13} cm^{-3} and gettered by phosphorus implantation at 550 °C, 650 °C, 750 °C and 850 °C for a cumulative time of 400 minutes. The experiments of FeB dissociation were carried out by using two standard intensities of 1 sun and 0.5 sun.

The findings showed that the dissociation rate increases by more than one order of magnitude when the level of iron contamination decreases from 1.2×10^{13} cm^{-3} to 7.2×10^{11} cm^{-3} under the effect of phosphorus implantation gettering. Contrary to R_d, the association rate R_a describing the accompanied phenomenon of dissociation remains almost constant and without showing a clear sensitivity to iron concentration. The effective time constant of FeB dissociation resulting from dissociation and association rates, has shown that the time required for a total dissociation of the FeB pairs becomes more shorter with the decrease of the iron content, on one hand, and the increase of the illumination intensity, on the other. The material constant K has also been determined. Its value was found to be $K = 1.4 \times 10^{-15}$ s. The study of repairing kinetics of FeB pairs after dissociation experiments led to the conclusion that the effective time constant of association is independent of iron concentration. It remains constant around 88 minutes.

Acknowledgements

This work is supported by General Directorate for Scientific Research and Technological Development (Algeria). The authors would like to acknowledge the provision of facilities and technical support by Aalto University at OtaNano – Micronova Nanofabrication Centre.

Received: ((will be filled in by the editorial staff))
Revised: ((will be filled in by the editorial staff))
Published online: ((will be filled in by the editorial staff))

References

[1] T. Buonassisi, A. A. Istratov, M. D. Pickett, M. Heuer, J. P. Kalejs, G. Hahn, M. A. Marcus, B. Lai, Z. Cai, S. M. Heald, T. F. Ciszek, R. F. Clark, D. W. Cunningham, A. M. Gabor, R. Jonczyk, S. Narayanan, E. Sauar, E. R. Weber, *Prog. Photovolt.: Res. Appl*. **2006**, 14, 513–531.

[2] S. Rein, S. W. Glunz, *J. Appl. Phys*. **2005**, 98, 113711.

[3] A.A. Istratov, H. Hieslmair, E.R. Weber, *Appl. Phys. A Mater. Sci. Process*. **2000**, 70, 489.

[4] A.A. Istratov, H. Hieslmair, E.R. Weber, *Appl. Phys. A Mater. Sci. Process*. **1999**, 69, 13.

[5] K. Graff and H. Pieper, *J. Electrochem. Soc*. **1981**, 128, 669.

[6] L. C. Kimerling and J. L. Benton, *Physica B & C* **1983**, 116B, 297.

[7] G. Zoth and W. Bergholz, *J. Appl. Phys.* **1990**, 67, 6764.

[8] X. Zhu, X. Yu, X. Li, P. Wang and D. Yang, *Scripta Materialia* **2011**, 64, pp. 217–220.

[9] D. Macdonald, T. Roth, P.N.K. Deenapanray, K. Bothe, P. Pohl, J. Schmidt, *J. Appl. Phys*. **2005**, 98, 083509.

[10] H. S. Laine, V. Vähänissi, Z. Liu, H. Huang, E. Magaña, A. E. Morishige, N. Khelifati, S. Husein, B. Lai, M. Bertoni, D. Bouhafs, T. Buonassisi, D. P. Fenning, H. Savin, in *Proc. 43rd IEEE Photovoltaic Specialists Conference (PVSC)*, Portland, OR, USA, 5-10 June **2016**.

[11] M. L. Polignano, D. Codegoni, S. Grasso, I. Mica, G. Borionetti, *Phys. Status Solidi A* **2015**, 212, No. 3, 495–505.

[12] D. Macdonald, L. J. Geerligs and A. Azzizi, *J. Appl. Phys.* **2004**, 95, pp. 1021-1028.

[13] K. Bothe, R. Sinton, an J. Schmidt, *Prog. Photovolt: Res. Appl.* **2005**, **13**, 287–296.

[14] K. Bothe and J. Schmidt, *J. Appl. Phys.* **2006**, 99, 013701.

[15] O. Palais, E. Yakimov, and S. Martinuzzi, *Mat. Sci. Eng. B*, **2002**, 91, 217.

[16] L. J. Geerligs and D. Macdonald, *Appl. Phys. Lett*. **2004**, 85, p. 5229.

[17] L. J. Geerligs, G. Coletti and D. Macdonald, in *Proc. 21st European Photovoltaic Solar Energy Conference (EUPVSEC)*, Dresden, Germany, **2006**.

[18] S. Herlufsen, D. Macdonald, K. Bothe, and J. Schmidt, *Phys. Status Solidi RRL* **2012**, 6, No. 1, p. 1–3.

[19] C. Möller, T. Bartel, F. Gibaja, and K. Lauer, *J. Appl. Phys.* **2014**, 116, 024503.

[20] C. Möller**,** A. Laades and K. Lauer, *Solid State Phenomena* **2014**, Vols. 205-206, pp 265-270.

[21] H. Reiss, C. S. Fuller, and F. J. Morin, *Bell Syst. Tech*. **1956**, J. 35, p. 535.

[22] J. Tan, D. Macdonald, F. Rougieux and A. Cuevas, *Semicond. Sci. Technol.* **2011**, 26, 055019.